

## Design and evaluation of an active secondary mirror positioning system for a small telescope

Andreas Sinn<sup>✉,\*</sup>, Patrik Prager<sup>✉</sup>, Christian Schwaer<sup>✉</sup>,  
and Georg Schitter<sup>✉</sup>

TU Wien, Automation and Control Institute (ACIN), Vienna, Austria

**Abstract.** This publication presents an active compensation system for the position of the secondary mirror of a small Ritchey–Chrétien telescope system. The goal is to maintain the optical imaging quality under varying gravitational and thermal influences, by compensation for the relative position deviations between the primary and secondary mirrors. An extensive analysis concerning the feasibility of such a system for a commercial off-the-shelf small telescope is performed and used as a basis for the design of the precision measurement and positioning system. The developed prototype uses dimensional metrology to capture relative position errors of the secondary mirror. A newly designed actuator with three degrees of freedom for the secondary mirror allows us to compensate for these deviations in a closed-loop control manner and ensures optimal positions of the two mirrors at all times. The support structure design requirements are reduced, allowing the utilization of more lightweight structures, as the artificial stiffness of the compensation system takes care of keeping the telescope mirrors in place. Furthermore, the measurement principle requires no light from the telescope, thus providing 100% of the collected light for the observation. The developed actuation and measurement principles are designed for simple scalability to larger representatives of small telescopes. The implemented setup is evaluated in various poses and temperature influences, successfully demonstrating that the calculated Strehl ratio is kept well above the diffraction limit of 80% for the used telescope system. © 2022 Society of Photo-Optical Instrumentation Engineers (SPIE) [DOI: [10.1117/1.JATIS.8.2.029007](https://doi.org/10.1117/1.JATIS.8.2.029007)]

**Keywords:** telescope system; system engineering; active secondary mirror; precision positioning.

Paper 21165G received Dec. 14, 2021; accepted for publication Jun. 3, 2022; published online Jun. 22, 2022.

### 1 Introduction

Small telescope systems (up to 1-m aperture) have proven themselves as a versatile tool in science. The vast amount of possible applications range from classical astronomical fields<sup>1,2</sup> over space debris observation,<sup>3–6</sup> free-space optical satellite communication<sup>7–10</sup> to SLR<sup>11,12</sup> as well as observation networks,<sup>13,14</sup> telescope arrays,<sup>15</sup> and fast-tracking of unmanned aerial vehicles (UAVs).<sup>16</sup> Independent of the application all telescope systems are susceptible to gravitational and thermal influences, as well as wind-shake and vibrations.<sup>17</sup> The first two reside in a low time constant regime, whereas the latter ones may range up to >100 Hz and are covered typically by means of adaptive optics.<sup>18</sup> Finite stiffness of the support structure/tube and the inherent temperature expansion cause deviations in the position and orientation of the secondary mirror with respect to the primary mirror. A key property of any telescope system is therefore to keep the alignment of the mirrors correctly for all operating conditions.

For many fields [e.g., optical satellite communication, satellite laser ranging, unmanned aerial vehicles (UAV) tracking] daylight operation introduces new challenges.<sup>3,19,20</sup> This is not only caused by the extended temperature operational range but also, e.g., by asymmetric exposure to direct radiation of the sun, resulting in thermal expansion and thus, skew of the structure.<sup>21</sup>

Active optics address the named problems by adding mechanisms that actively (re-)position or deform system components to maintain correct alignment and surface shapes.<sup>18</sup> Large telescopes typically require an active support of the primary mirror in addition to a secondary mirror

\*Address all correspondence to Andreas Sinn, [sinn@acin.tuwien.ac.at](mailto:sinn@acin.tuwien.ac.at)

2329-4124/2022/\$28.00 © 2022 SPIE

Sinn et al.: Design and evaluation of an active secondary mirror positioning system for a small telescope

positioning system.<sup>22–24</sup> Mirrors of small telescopes typically have lower aspect ratios and therefore, are only susceptible to deviations from the ideal positions. To ensure the correct position of the secondary mirror, various approaches such as Stewart platforms<sup>25–27</sup> and active structures<sup>28,29</sup> have been demonstrated successfully in literature. Most of these systems use five degrees of freedom (DoF) for the secondary mirror, which adds benefits during mirror alignment. However, also three DoF are used, e.g., in the New Technology Telescope (NTT).<sup>30</sup>

Small telescope systems have not been covered as extensively in literature but recently have gained more attention in active optics.<sup>31,32</sup> Active positioning of the secondary mirror in this telescope class is typically used to integrate the focusing mechanism (one DoF) into the telescope,<sup>33</sup> but up to six DoF have been proposed.<sup>34</sup> With respect to daylight operation small telescope systems may be limited in their achievable performance by the ambient temperature and direct (and indirect, if the telescope is enclosed somehow) sun radiation conditions. Furthermore, due to the resulting error amplitude of these disturbances many adaptive optical systems require a precompensated, well-focused telescope to achieve their full potential.<sup>35</sup> Open-loop compensation of environmental influences is possible and typically relies on ambient and mirror temperature, as well as the zenith angle.<sup>29</sup> However, especially asymmetric thermal influences would require a large number of sensors and extensive calibration to achieve similar performance as closed-loop operation.

The contribution of this publication is a system that compensates for the relative position between the secondary and primary mirror of a small telescope system, to maintain a high imaging quality under environmental influences such as gravity and thermal exposure. Dimensional metrology is applied to capture the relative mirror position, hence, requiring no light from the telescope. The proposed approach increases the stiffness of the telescope structure artificially using feedback control, enabling more lightweight structures and simple scalability for larger telescope systems. A commercial off-the-shelf (COTS) 25-cm Ritchey–Chrétien-telescope (RC-telescope) with truss structure is used as representative of a typical telescope design for small systems. The impact of gravity and temperature fluctuations is analyzed and determines the DoF and motion ranges of the actuator to study the feasibility of the suggested approach.

## 2 System Concept and Requirements

The main idea of the proposed approach is to ensure constant imaging quality in presence of thermal and gravitational disturbances, by artificially increasing the stiffness of the support structure using feedback control. The relative position between the secondary and the primary mirror is measured and deviations are corrected by means of an active mount of the secondary mirror. This ensures that the designed, optimal position of the secondary is maintained and aberrations due to mirror misalignment are suppressed.

Figure 1 presents the main components of the proposed system and their location in the telescope. A dimensional measurement system (interferometer) and an actuation system for

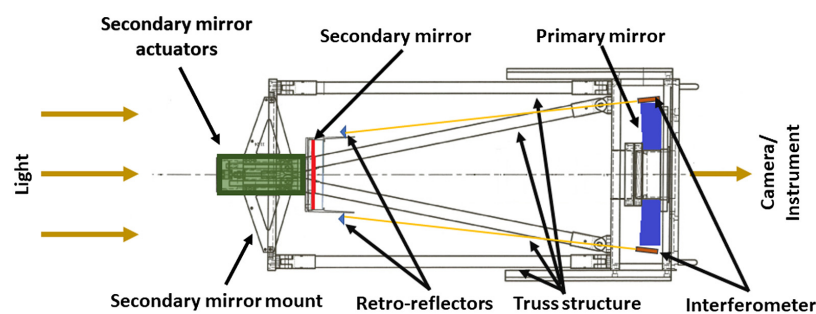


**Fig. 1** Illustration of the proposed system concept. A dimensional measurement system tracks the relative position of the secondary mirror and compensates for deviations by means of an active secondary mount to maintain correct mirror alignment.

Sinn et al.: Design and evaluation of an active secondary mirror positioning system for a small telescope

the secondary mirror are integrated into a small COTS RC-telescope. To determine the requirements for the measurement and the actuators for the secondary mirror, finite element (FE) analysis and optical ray-tracing are used in combination with measurements on the implemented system. The details and results are described in the following sections.

## 2.1 Finite Element Model-Based Evaluation

A FE model of the 25-cm telescope is created and used to study various environmental influences onto the relative position between the secondary and the primary mirror in simulation. The model is a simplification of the used telescope system, as the main intention of this evaluation is the analysis of a truss structure and its behavior. Therefore, the ball joints are modeled ideally, the primary mirror alignment mechanism is neglected and perfect symmetry of the components is assumed. These simplifications are justified as the proposed closed-loop system would compensate for the reduced stiffness due to the named reasons, as well as for asymmetric displacements.

Aluminum is used for all metal components of the telescope. As the exact properties of the rods of the truss structure made of carbon-fiber-reinforced polymers (CFRP) are not specified by the manufacturer, values from literature<sup>36</sup> are taken for the mechanical behavior. A measurement of the thermal expansion coefficient is conducted using a similar setup to the one described in Sec. 3.1. It is found to be  $\approx 2.1 \cdot 10^{-6} \text{ K}^{-1}$  in the relevant temperature range.

Static simulations in SolidWorks (Dassault Systèmes, Stuttgart, Germany) allow the analysis of gravitational as well as thermal influences. The telescope in vertical position (90-deg elevation) including gravity is used as a reference, where all position deviations are considered to be zero (ideal alignment of secondary and primary mirror). Then the gravity vector is applied in various directions and the resulting relative displacements are recorded. The impact of gravity as shown exemplarily in Fig. 2(a) at 0-deg elevation is especially visible in tilt and lateral displacement, both due to bending of the supporting structure.

The impact of homogeneous temperature changes is evaluated at different temperatures and thermal equilibrium using static simulations in SolidWorks. They are conducted in the reference position and meet the expected behavior of axial displacement only. Due to the length of the telescope ( $\approx 600 \text{ mm}$ ) and the resulting thermal expansion, this is one of the largest displacements (Table 1) caused by external influences.

The analysis of the asymmetric temperature increase of the structure [as indicated in Fig. 2(b)] is performed in a similar way, but the temperature changes are only applied to one side of the telescope. The rods shaded with a chessboard pattern are set to a temperature of 30°C above the remaining of the telescope. This corresponds well with the asymmetric thermal disturbance applied for experimental verification in Sec. 4.2. The disturbance causes tilt, axial, and lateral displacement and has, compared with gravity, significantly more impact on the relative position between the primary and secondary mirrors.

In summary, the investigated small telescope (<30 cm) with truss structure may be considered insensitive to gravity, due to the usage of optimized materials (CFRP) and structures

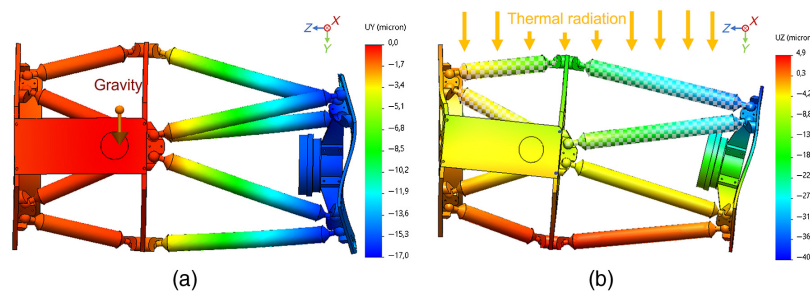


**Fig. 2** Simulation analysis for gravitational and temperature influence (deformations exaggerated): (a) Displacement in  $y$ -direction due to gravity for 0-deg elevation. (b) Nonuniform temperature intake (+30°C) and resulting displacement in (axial)  $z$ -direction.

Sinn et al.: Design and evaluation of an active secondary mirror positioning system for a small telescope

**Table 1** Results of the mechanical system analysis and the corresponding optical performance of the telescope. The two remaining DoF (tip and orthogonal lateral) show no significant deviations.

Disturbance	Amount	Tilt ( $\mu\text{rad}$ )	Axial ( $\mu\text{m}$ )	Lateral ( $\mu\text{m}$ )	RMS WFE (nm)	Strehl (%)
Gravity	45-deg elev.	6.5	2.5	10.4	11.2	98.4
Gravity	0-deg elev.	18.2	0.18	16.7	0.9	99.9
Asymmetric thermal	+30°C	176.8	34.4	28.7	153.2	<10
Homogeneous thermal	$\pm 25^\circ\text{C}$	0.0	$\pm 26.1$	0	116.5	<10
Asym. therm., gravity	+30°C and 45-deg	183.0	45.9	41.1	204.6	<10

(e.g., truss or Serrurier truss). However, larger telescopes imply heavier mirrors and supporting structures (mass increases disproportionately with primary mirror diameter), increasing the impact of gravity onto the relative mirror position. Furthermore, thermal performance may be limiting with regard to the new challenges introduced by daylight operation. Although the thermal expansion coefficient of CFRP elements is small, thermal exposure still affects the relative position of the mirrors considerably.

## 2.2 Optical Analysis

To quantify the influence of mechanical and thermal behavior in terms of optical performance, a simulation in OpticStudio (Zemax LLC, Washington, United States) is performed. A model of the telescope [shown in Fig. 3(a)] is derived from the specification given by the manufacturer (Table 2) following a classical RC-telescope design approach.<sup>37</sup> The optical performance is evaluated in terms of RMS wavefront error (WFE) and resulting Strehl ratio at a wavelength of 550 nm. It depends on three DoF (due to rotational symmetry): (1) mirror tilt, (2) lateral decenter from the optical axis, and (3) axial displacement along the optical axis. The results from the FE-analysis (Table 1) are applied in OpticStudio and the resulting errors are discussed. Gravity has only little effect on the RMS WFE and a Strehl ratio of well above 98% is maintained in all poses. For sensitive applications, using more material for the structure and consequently increasing the stiffness may reduce these errors further.

For the thermal disturbance cases, the impact on the WFE is significantly larger, reducing the Strehl ratio to below 10% in the case of homogeneous temperature changes (ambient temperature range from  $-5^\circ\text{C}$  to  $45^\circ\text{C}$ ) due to a high amount of defocus. Although defocus is typically compensated externally due to its pure geometric nature, some kind of quality measure including

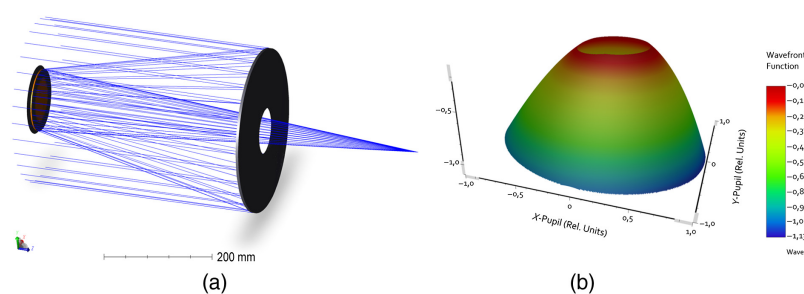


**Fig. 3** Ray tracing results acquired using OpticStudio: (a) Optical layout of the 25-cm RC-telescope. (b) Wavefront map for an asymmetric thermal disturbance of 30°C. A clear dominance of defocus is visible.

Sinn et al.: Design and evaluation of an active secondary mirror positioning system for a small telescope

**Table 2** GSO 25-cm RC-Telescope specification including derived properties (bottom) used for the optical system analysis in OpticStudio.

Property	Value
Primary diameter	254 mm
Secondary diameter	109 mm
Focal length	2000 mm
Back focal distance <sup>a</sup>	747.5 mm
Primary-secondary distance <sup>a</sup>	-441.6 mm
Primary radius	-1410.4 mm
Secondary radius	-814.357 mm
Primary conic constant	-1.148
Secondary conic constant	-5.829

<sup>a</sup>Measured quantity.

a sensor (e.g., spot size) is required to determine the optimal position, which is not readily available for all scientific instruments.

Furthermore, asymmetric thermal exposure lowers the achievable Strehl ratio and is caused by a mixture of aberrations [coma, astigmatism, and defocus, depicted in Fig. 3(b)]. In terms of diffraction-limited imaging quality of the telescope (Strehl > 80%<sup>37</sup>) the analyzed telescope system is already significantly below this limit. As both cases become worse for larger and optically faster telescopes, an active compensation system is required, to maintain the optimum relative position between the primary and secondary mirrors in the presence of gravitational and thermal disturbances.

It is emphasized that the presented WFE and Strehl ratios are calculated using OpticStudio from the measured position deviations only, and other errors such as mirror shape imperfections, initial misalignment, and seeing are not taken into account for this publication.

### 2.3 Requirements

For full compensation of the observed position deviations between the primary and secondary mirrors five DoF are required. In large telescope systems, these DoF are typically covered by a hexapod.<sup>26</sup> However, for small telescope systems, this approach may not be applicable due to volume and weight restrictions,<sup>38</sup> as well as for cost-efficiency reasons. From all deviations, lateral decenter allows comparably large values, e.g., 250  $\mu\text{m}$  to maintain a Strehl ratio of 80%, whereas for axial displacement only 10  $\mu\text{m}$  and for tilt 0.960 mrad are possible. As the results from the mechanical system analysis indicate a worst-case lateral shift of only 42  $\mu\text{m}$  (at 45-deg elevation and asymmetric temperature of +30°C, Table 1), resulting in a Strehl ratio of 99.0%, lateral shift is neglected for the proposed system. Hence, the required number of measured and compensated DoF is reduced to three (tip, tilt, and axial displacement). This significantly lowers the system volume as well as complexity, enabling a compact and integrated design of the active compensation system.

With respect to the system analysis and the potential future applicability in larger telescopes (up to 80-cm primary mirror diameter), the requirements for the compensation system are  $\pm 0.436$  mrad tip/tilt actuation range and  $\pm 100$   $\mu\text{m}$  axial displacement range. For a typical satellite tracking velocity of 3 degrees per second (dps) and an elevation range of 90 deg, a minimum target bandwidth of 0.5 Hz is targeted for the compensation system to achieve at least 20-dB disturbance rejection. An elevation range from 0 deg to 90 deg is chosen as worst case setting to include the extreme positions (zenith and horizon) in the investigation, as an application such as UAV tracking has a typical main operating range of 0 deg to 30 deg.

Sinn et al.: Design and evaluation of an active secondary mirror positioning system for a small telescope

### 3 System Design

Using the requirements from the previous sections the individual components of the compensation system are designed and described in the following subsections.

#### 3.1 Metrology System

To determine the position of the secondary with respect to the primary mirror, a three-DoF dimensional metrology system based on an Attocube interferometer with three long-range sensor heads (IDS3010 and M12/C7.6 heads, Attocube Systems AG, Haar, Germany) is implemented. Therefore, no light from the telescope is required for the proposed approach. The sensor heads are mounted in a 120-deg pattern directly to the primary mirror circumference (placed on a circle with 135-mm radius) using high-strength epoxy and point toward the front of the telescope (Fig. 1). They are aligned pairwise to retroreflectors that are attached to the secondary mirror mount (retroreflector centers on a circle with 85-mm radius) resulting in a nominal measurement distance of 430.9 mm. The measurement outputs of the interferometer are transmitted digitally via a high-speed serial link to the real-time hardware where tip and tilt angles of the secondary, as well as displacement along the optical axis, are calculated for analysis using basic geometry.

However, other sensing principles (e.g., optical triangulation sensors) could be utilized for the proposed system, as the used interferometer exceeds the requirements in terms of measurement resolution and bandwidth significantly.

#### 3.2 Actuator Design

Based on the requirements developed in Sec. 2.3, an actuation system for three DoF is developed. The basic structure of the proposed actuator is shown in Fig. 4(a). An approach with two flexures and a linear bearing was chosen for defined stiffness and motion ranges. A key design constraint is to achieve a compact design, which does not require a larger cross-section than the obstruction of the secondary mirror. The main flexure is a two-axis notch flexure for tip-tilt motion, which is located right behind the secondary mirror. It is rotationally symmetric and provides the same stiffness in tip and tilt direction. The linear bearing (highlighted in green) guides the mover in axial direction and ensures tip-tilt movement around the notch flexure only. An additional membrane flexure on the back of the actuator body defines the axial stiffness, compensates the weight of the secondary mirror and prevents rotation around the optical axis. Both flexures are designed to have the first modes (suspension modes) above 30 Hz, providing sufficient margin to the target control bandwidth of up to several Hertz.

Three COTS Lorentz actuators (VCAR0044-0075-00A, SUPT Motion, Jangsu, China) with custom-made PWM-current amplifiers enable displacement and tip-tilt motion of the secondary mirror. The stiffnesses of the flexures together with the maximum force of the Lorentz actuators enable a motion range in accordance with the system requirements. They are arranged in

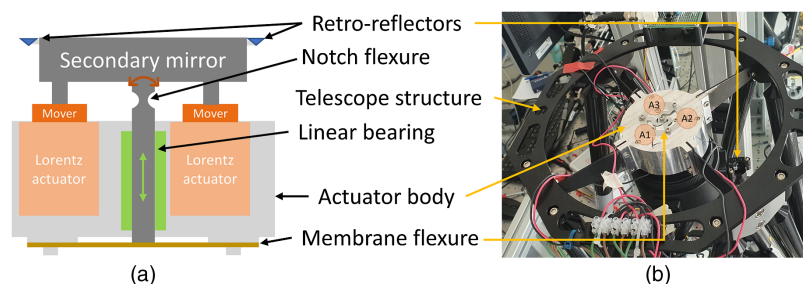


**Fig. 4** Details of the developed 3-DoF actuator: (a) Cross-section showing the Lorentz actuators and the flexures. (b) Actuator assembly in the modified 25-cm RC-telescope.

Sinn et al.: Design and evaluation of an active secondary mirror positioning system for a small telescope

a 120-deg pattern, which is coaligned to the sensor pattern, enabling pairwise allocation of opposite sensors and actuators for feedback control.

#### 4 Implementation and Experimental Verification

To evaluate the feasibility of the proposed system, a 25-cm RC telescope (GSO RC 254/2000, Guang Sheng Optical, Taiwan) with a truss structure is modified. An overview is given in Fig. 5. The secondary mirror mount is replaced by the designed actuator body. The spider assembly and secondary mirror position are kept as in the original system. The telescope system is mounted using a fork mount in alt-az configuration, which is typical for satellite tracking applications.<sup>39</sup> An accelerometer provides a measurement of the elevation angle, which provides sufficient accuracy (1 deg) for estimation of the telescope pose for this publication but is not intended for on-sky operation since the required telescope mount is usually equipped with high-resolution encoders. The full system is operated on a vibration isolation table, reducing the impact of ground vibrations onto the measurements. A MicroLabBox (dSpace GmbH, Paderborn, Germany) is used as real-time hardware for signal acquisition and feedback control with a sampling frequency of 10 kHz and PWM output to the actuator drivers.

As intended, the system response (Fig. 6) shows no significant dynamic behavior until the first resonance (tip-tilt mode) at  $\sim 27$  Hz. The second resonance peak results from the membrane flexure. As the target closed-loop bandwidth is in the range of single Hertz, the actuator will be used on the spring line of the system only. Furthermore, the crosstalk (Fig. 6) of all axes at small frequencies is at least 10 dB below the corresponding spring line of the system dynamics (pairs of opposite sensor and actuators). Hence, this crosstalk may be neglected as its undesired influence is small and the controller design is reduced to the tuning of three independent SISO systems, implemented as proportional-integral (PI)-controllers and designed for a closed-loop bandwidth of 3 Hz (60-deg phase margin).<sup>40</sup>

##### 4.1 Gravitational Influence

Gravitational influence onto the telescope structure is investigated by slewing the telescope including the developed actuator manually from an elevation angle of 90 deg to 0 deg. A fast trajectory with a maximum velocity of around 3 dps is chosen to evaluate the system under the influence of rapidly changing direction of gravity, as experienced in satellite and UAV tracking. The relative position offsets with respect to the vertical reference pose are recorded during this process. The corresponding tip, tilt, and  $z$ -displacement errors are calculated for comparison to the system analysis in postprocessing.

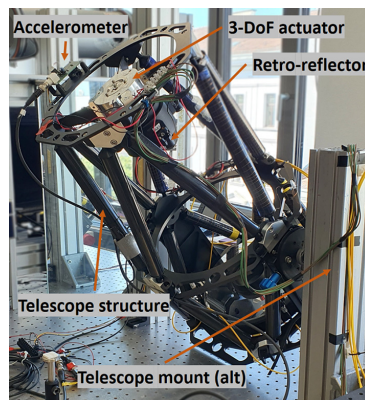


**Fig. 5** Developed system in alt-az configuration. An elevation range of 0 deg to 90 deg is possible.

Sinn et al.: Design and evaluation of an active secondary mirror positioning system for a small telescope

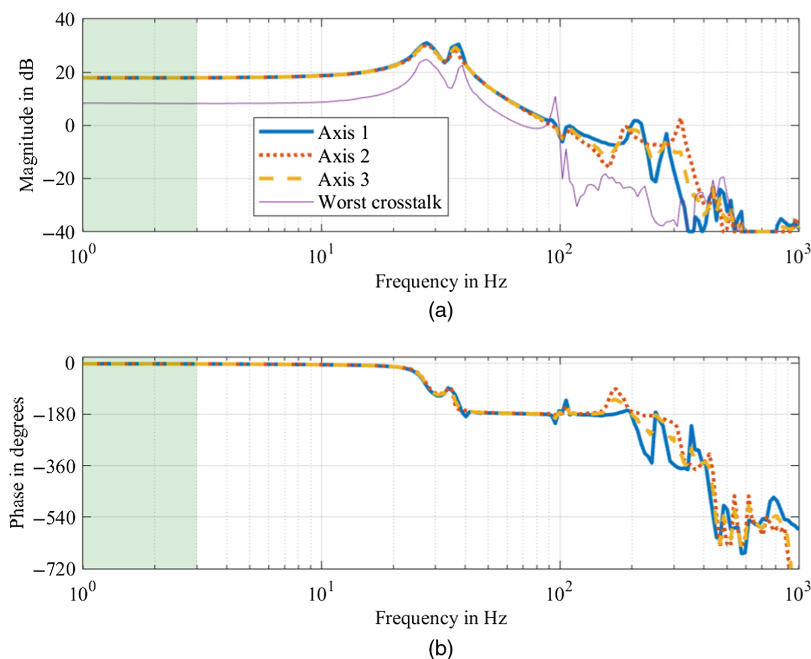


**Fig. 6** Bode plots of dynamic response of the sensor-actuator pairs at 45-deg elevation showing the first resonance (tip-tilt flexure) at 27.3 Hz. The dynamic behavior of the three axes agrees well and no dynamics are observed in the target bandwidth range of up to 3 Hz (highlighted by green background). The worst-case crosstalk between the axes is indicated by the purple line.

Two slews are compared: One without compensation and fixed flexures (representing the original system) depicted in Fig. 7(a) and one with active compensation of the relative mirror position shown in Fig. 7(b). The measured elevation angle over time (top), as well as the tilt-velocity is shown for reference purpose. Without compensation, a small dependency of all DoF to gravity is visible in the measured errors (center left). Tilt dominates the error because this axis is co-aligned to the altitude axis of the telescope. Tip is present due to asymmetries of the assembled system. In comparison to the mechanical system analysis, the measured tilt deviations are higher but their total effect on the resulting Strehl ratio (>98%) is, as expected, low. However, for larger telescopes or more lightweight structures gravitational influence is more prominent.

With active compensation of the position of the secondary mirror, all errors are kept close to zero over the full elevation range [Fig. 7(b)]. The RMS WFE is reduced by a factor of 33 to 0.64 nm (2.0 nm max.), resulting in a calculated Strehl ratio of 99.9%. Table 3 summarizes the measurements in terms of RMS and maximum position errors and presents the corresponding Strehl ratios for each case. The gravitational influence is now visible in the controller outputs for the Lorentz actuators only. Due to the orientation of the three actuators with respect to the altitude axis, actuators 1 and 3 push, and actuator 2 pulls as intended. The controller output values stay below 20% of the maximum current, leaving sufficient margin for up-scaling of the system to larger telescopes.

The influence of increased weight of the secondary mirror unit due to the developed precision positioning system is not considered to be an issue. A measurement without compensation from 90 deg to 0 deg elevation with additional weight ( $\approx 0.5$  kg) attached to the spider indicates a change of the resulting Strehl ratio of <2%, and the proposed system is able to compensate for this influence.

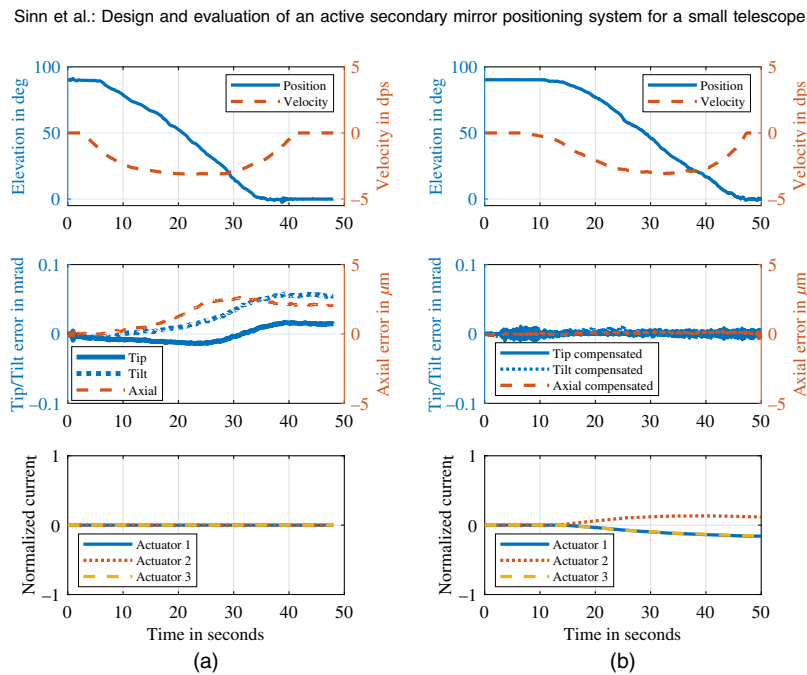


**Fig. 7** System behavior over varying elevation angles. (a) Without compensation (original system) and (b) With active compensation of secondary mirror position. A clear reduction of all errors (tip, tilt, and axial displacement) is visible in the right-center plot.

**Table 3** Measurement results and comparison of the feedback controlled to the uncompensated system for gravitational (top) and thermal (bottom) influences. The output of the three interferometer axes (relative displacement) and the thereof calculated relative position errors (tip, tilt, and axial displacement) of the secondary mirror are shown.

	Relative displacement			Relative position error			Strehl ratio <sup>a</sup> (%)
	Axis 1 (μm)	Axis 2 (μm)	Axis 3 (μm)	Tip (μrad)	Tilt (μrad)	Axial (μm)	
Tilt of the telescope from 90 deg to 0 deg elevation over 40 s							
No compensation (RMS)	1.009	3.912	1.398	10.75	33.44	1.723	99.0
No compensation (max)	1.697	5.601	2.720	16.47	58.10	2.628	98.2
Compensated (RMS)	0.223	0.234	0.197	1.92	3.70	0.085	100.0
Compensated (max)	0.709	0.917	0.538	11.39	10.95	0.400	99.9
Asymmetric temperature increase by 30°C over 5 min							
No compensation (RMS)	18.287	38.861	27.129	60.62	110.74	28.152	12.8
No compensation (max)	25.759	56.541	39.553	101.42	157.90	40.523	<10
Compensated (RMS)	0.066	0.081	0.064	1.48	1.19	0.040	100.0
Compensated (max)	0.508	0.726	0.615	7.64	6.36	0.232	100.0

<sup>a</sup>The Strehl ratio is calculated from the residual position errors only and neglects other, e.g., mirror imperfections).

Sinn et al.: Design and evaluation of an active secondary mirror positioning system for a small telescope

#### 4.2 Thermal Behavior

The influence of temperature variations is measured in a similar manner as gravitational influence. Instead of tilting the telescope, a resistive wire is wound around the rods of the truss structure [selected rods are indicated by a chessboard pattern in Fig. 2(b)] and heated by an electric current to simulate an asymmetric exposure of the telescope structure to thermal radiation. A temperature increase of  $+30^{\circ}\text{C}$  is applied to half of the structure of the telescope in vertical position (90-deg elevation). This increase simulates temperature change due to direct sunlight onto the telescope system. The thermal behavior is characterized without compensation and fixed flexures [Fig. 8(a)] and with active compensation by the proposed system [Fig. 8(b)]. Without compensation, a clear correlation between temperature and measured errors is visible in all three DoF. The measured amount of tilt meets the expectations from the thermal simulations. Tip is introduced due to differences in the applied temperature distribution, as well as variations of the thermal expansion coefficient. The RMS value of the measured deviations over the full measurement duration leads to a calculated WFE of 125-nm RMS (181 nm max.), which is equivalent to a Strehl ratio of 13% (max:  $<10\%$ ).

Active feedback control effectively compensates for the impact of asymmetric thermal exposure, reducing the residual error to the noise floor of the current amplifiers. This results in a reduction of the RMS WFE by a factor of 250 to 0.49 nm (1.25 nm max.), corresponding to a calculated Strehl ratio of 100%. The normalized currents indicate a utilization of  $<10\%$  of the maximum current, leaving sufficient margin for compensation of other (gravitational) disturbances, as well as room for scalability.

Measurements of the response related to homogeneous temperature changes of the full telescope system (e.g., due to ambient temperature variations) are not executed, but the compensation principle is the same for this type of disturbance.

For evaluating the full axial displacement, a constant reference input signal (chosen to achieve 100% normalized output current) is applied to all three control loops and the axial

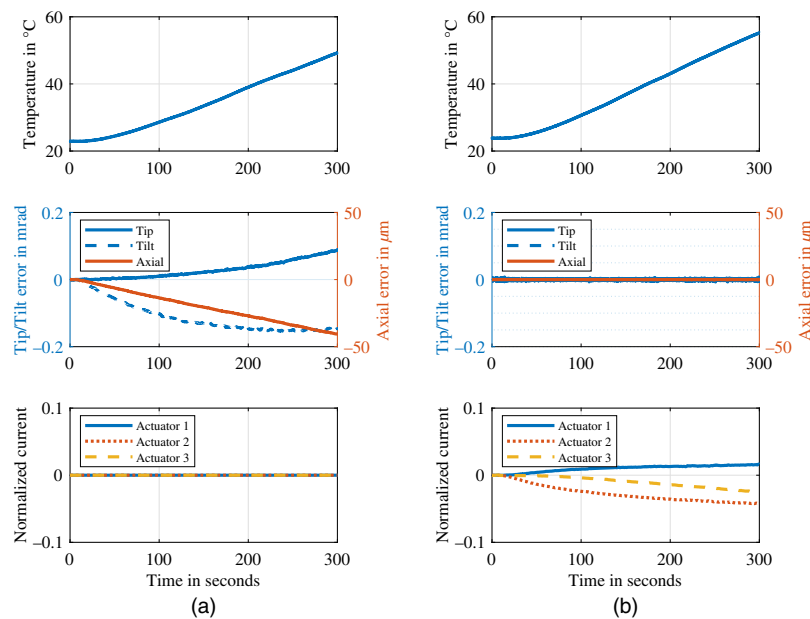


**Fig. 8** System behavior under asymmetric temperature exposure. (a) Without compensation (original system). (b) With active compensation of secondary mirror position. The remaining error is reduced significantly over the temperature change of  $30^{\circ}\text{C}$ .

Sinn et al.: Design and evaluation of an active secondary mirror positioning system for a small telescope

displacement is acquired, indicating a maximum axial displacement of  $\pm 200 \mu\text{m}$ , which exceeds the required range derived in Sec. 2. Therefore, axial displacement due to homogeneous thermal expansion is considered to be covered by the proposed system.

The residual RMS WFE with compensation is slightly larger in the gravitational case because mechanical vibrations exceeding the compensation bandwidth of 3 Hz are introduced by manual slewing of the telescope. However, the minimum bandwidth requirement of 0.5 Hz, which results from maximum slewing velocities of 3 dps, is met.

In summary, both gravitational and thermal influences have measurable impact on the optical performance of the telescope. With regard to larger telescopes (up to 80 cm) and especially optically faster telescopes, where the effect of these disturbances is even more prominent, an active compensation system may be highly beneficial. Using the relative displacement values presented in Table 3, which characterize the residual position uncertainty of the individual sensor-actuator pairs, the performance of the proposed compensation system applied in other telescopes can be estimated. With the proposed position compensation system, a calculated Strehl ratio of  $>99\%$  is maintained during gravitational as well as thermal influences, effectively proving the feasibility and applicability of an active secondary mirror for a small telescope system.

## 5 Conclusion

This publication investigates the feasibility of an active compensation system for positioning the secondary mirror in a small telescope to maintain high imaging quality in the presence of gravitational and thermal disturbances. Based on an optomechanical system analysis, a precision positioning system is developed and integrated into a small, 25-cm COTS RC-telescope. Dimensional metrology is used to determine the relative position of the primary and secondary mirror, hence, no light from the application is required. Feedback control of three DoF (tip, tilt, and axial displacement of the secondary mirror) with a bandwidth of 3 Hz enables a reduction by a respective factor of 33 for gravitational and 250 for asymmetric thermal disturbances. A calculated Strehl ratio of well above 80% is maintained for all measured operating conditions, successfully demonstrating the feasibility of the proposed approach. The system is designed to be scaled to larger telescope systems up to 80 cm providing its benefits to various applications and telescope sizes. This increases the design freedom for the telescope support structure (e.g., reduced stiffness requirements) and especially enables more lightweight construction approaches.

Next steps include an increase of the control bandwidth to allow compensation of low-frequency vibrations and the integration of a wavefront sensor for on-sky verification of the optical performance.

## Acknowledgments

This work was funded by the Hochschuljubilaeumsfonds of the city of Vienna, Austria under the project number H-220966/2018 and by the Austrian Research Promotion Agency (FFG) under the scope of the Austrian Space Applications Programme (ASAP), contract number 873711. The authors declare that they have no known competing financial interests or personal relationships that could have appeared to influence the work reported in this paper.

## References

1. T. Oswalt, *The Future of Small Telescopes in the New Millennium*, 1st ed., Springer, Dordrecht (2003).
2. F. Ringwald et al., "The research productivity of small telescopes and space telescopes," arXiv:Astrophysics, no. astro-ph/0309772 (2003).
3. M. A. Steindorfer et al., "Daylight space debris laser ranging," *Nat. Commun.* **11**(1), 2–5 (2020).

Sinn et al.: Design and evaluation of an active secondary mirror positioning system for a small telescope

4. S. Schmalz et al., "ISON's sub-network of small aperture telescopes for observations of NEOs, space debris and meteors," in *1st NEO and Debris Detect. Conf.* (2019).
5. J. Šilha, "Small telescopes and their application in space debris research and space surveillance tracking," *Contrib. Astron. Obs. Skalnaté Pleso* **49**(2), 307–319 (2019).
6. M. Ploner et al., "Ultrafast wide field telescope for space debris detection and tracking," in *Proc. Adv. Maui Opt. and Space Surveill. Technol. Conf.* (2019).
7. S. K. Liao et al., "Satellite-relayed intercontinental quantum network," *Phys. Rev. Lett.* **120**, 030501 (2018).
8. A. Shrestha and M. Brechtelsbauer, "Transportable optical ground station for high-speed free-space laser communication," *Proc. SPIE* **8517**, 851706 (2012).
9. C. Fuchs et al., "SOTA optical downlinks to DLR's optical ground stations," *Proc. SPIE* **10562**, 1056247 (2017).
10. K. Riesing, H. Yoon, and K. Cahoy, "A portable optical ground station for low-earth orbit satellite communications," in *Proc. IEEE Int. Conf. Space Opt. Syst. and Appl.*, pp. 118–124 (2017).
11. P. Wang et al., "Megahertz repetition rate satellite laser ranging demonstration at Graz observatory," *Opt. Lett.* **46**, 937–940 (2021).
12. J. F. McGarry et al., "NASA's satellite laser ranging systems for the 21st century," *J. Geod.* **93**, 2249–2262 (2019).
13. F. K. Chun et al., "A new global array of optical telescopes: the falcon telescope network," *Publ. Astron. Soc. Pac.* **130**(991), 095003 (2018).
14. P. Gebhardt et al., "U-SMART: small aperture robotic telescopes for universities," *Rev. Mexicana Astron. Astrofísica: Ser. Conf.* **51**, 44–46 (2017).
15. M. J. Creech-Eakman et al., "Magdalena ridge observatory interferometer: 2014 status update," *Proc. SPIE* **9146**, 91460H (2014).
16. D. Ojdic et al., "UAV detection and tracking with a robotic telescope system," in *IEEE/ASME AIM 2021* (2021).
17. R. Wilson, *Reflecting Telescope Optics II*, 1st ed., Springer-Verlag, Berlin Heidelberg (1999).
18. H. W. Babcock, "The possibility of compensating astronomical seeing," *Publ. Astron. Soc. Pac.* **65**(386), 229–236 (1953).
19. H. Kaushal and G. Kaddoum, "Free space optical communication: challenges and mitigation techniques," *IEEE Commun. Surv. Tutor.* **19**(1), 57–96 (2017).
20. M. P. Peloso et al., "Daylight operation of a free space, entanglement-based quantum key distribution system," *New J. Phys.* **11**(4), 045007 (2009).
21. P. L. Tsela, L. Combrinck, and B. Ngcobo, "A spatiotemporal analysis of the effect of ambient temperatures on the thermal behaviour of the Lunar Laser Ranging optical telescope at Hartebeesthoek Radio Astronomy Observatory," *South Afr. J. Geomat.* **5**(3), 373 (2016).
22. R. N. Wilson, F. Franza, and L. Noethe, "Active optics I. A system for optimizing the optical quality and reducing the costs of large telescopes," *J. Mod. Opt.* **34**(4), 485–509 (1987).
23. P. Wizinowich et al., "Optical quality of the W.M. Keck Telescope," *Proc. SPIE* **2199**, 94–104 (1994).
24. S. Guisard, L. Noethe, and J. Spyromilio, "Performance of active optics at the VLT," *Proc. SPIE* **4003**, 154–164 (2000).
25. F. Bortoletto et al., "An active telescope secondary mirror control system," *Rev. Sci. Instrum.* **70**, 2856 (1999).
26. P. Schipani et al., "Active optics control of VST telescope secondary mirror," *Appl. Opt.* **49**(16), 3199–3207 (2010).
27. P. Schipani et al., "Active optics system of the VLT Survey Telescope," *Appl. Opt.* **55**(7), 1573–1583 (2016).
28. N. Roddier et al., "The WIYN telescope active optics system," *Proc. SPIE* **2479**, 364–376 (1995).
29. B. Smith et al., "The active optics system for the discovery channel telescope," *Proc. SPIE* **7739**, 77391T (2010).
30. L. Noethe, "Active optics in modern, large optical telescopes," *Prog. Opt.* **43**, 1–69 (2002).

Sinn et al.: Design and evaluation of an active secondary mirror positioning system for a small telescope

31. C. Schwaer et al., "Design methodology to develop an active optics system for a thin 1-m meniscus mirror," *J. Astron. Telesc. Instrum. Syst.* **6**(4), 049002 (2020).
32. D. S. Niu, G. M. Wang, and B. Z. Gu, "Active support system for 1-m SONG primary mirror," *J. Instrum.* **7**, T05001 (2012).
33. ASA Astrosysteme GmbH, "ASA cassegrain systems," Product folder (2021).
34. R. Wang et al., "Precision analysis and error compensation of a telescope truss structure based on robotics," *Appl. Sci. (Switzerland)* **10**(18), 6424 (2020).
35. J.-M. Delvit et al., "Wave front sensing for next generation earth observation telescope," *Proc. SPIE* **10562**, 105625H (2017).
36. ACP Composites, "Mechanical properties of carbon fiber composite materials, fiber/epoxy resin," Product specification (2014).
37. R. N. Wilson, *Reflecting Telescope Optics I*, 2nd ed., Springer (2007).
38. L. Zago and S. Droz, "A small parallel manipulator for the active alignment and focusing of the secondary mirror of the VLTI ATS," *Proc. SPIE* **4003**, 450–455 (2000).
39. T. Riel et al., "High performance motion control for optical satellite tracking systems," *Adv. Space Res.* **65**(5), 1333–1343 (2020).
40. R. Munning Schmidt et al., *The Design of High Performance Mechatronics*, 3rd ed., Delft University Press (2020).

**Andreas Sinn** is a doctoral researcher at the Automation and Control Institute (ACIN), group for Advanced Mechatronic Systems (AMS) at TU Wien, Vienna, Austria. He received his MSc degree in electrical engineering from TU Wien in 2016. His primary research interests are adaptive optics and system integration for optical ground stations, as well as high-performance telescope systems for object tracking and identification.

**Patrik Prager** completed his master's degree at the Automation and Control Institute (ACIN), group for Advanced Mechatronic Systems (AMS) at TU Wien, Vienna, Austria, in November 2021. He received his BSc degree in electrical engineering from TU Wien in 2017. His primary research interests are in precision engineering, system integration, and active optics for telescope systems.

**Christian Schwaer** is a PhD student at the Automation and Control Institute (ACIN) of TU Wien. He received his MSc degree in mechanical engineering with specialization in automation and information technology from Karlsruhe Institute of Technology, Germany, in 2017. His primary research interests include high-performance mechatronic systems, system integration, control concepts, and their application in optical systems.

**Georg Schitter** is a professor for advanced mechatronic systems at the Automation and Control Institute (ACIN) of TU Wien. He received his MSc degree in electrical engineering from TU Graz, Austria (2000) and his MSc and PhD degrees from ETH Zurich, Switzerland (2004). His primary research interests are in high-performance mechatronic systems, particularly for applications in the high-tech industry, scientific instrumentation, and mechatronic imaging systems, such as AFM, scanning laser and LIDAR systems, telescope systems, adaptive optics, and lithography systems for semiconductor industry.